  Bull. Chem. Soc. Jpn., 56, 405—411 (1983)

Electronic Spectra and Crystal Structure of Organic Radical Salt: Dimethyldibenzotetrathiafulvalenium Tetrafluoroborate

Chizuko TANAKA,* Jiro TANAKA, Karlheinz DIETZ,†† Chuji KATAYAMA, and Masashi TANAKA†

Department of Chemistry, Faculty of Science, Nagoya University, Chikusa-ku, Nagoya 464

†*College of General Education, Nagoya University, Chikusa-ku, Nagoya 464*

(Received August 16, 1982)

The single crystal of dimethyldibenzotetrathiafulvalenium tetrafluoroborate (1 : 1) has been prepared by electrocrystallization. The crystal structure has been determined by X-ray crystal analysis. The salt crystallizes in Ibam with $a=14.637(3)$, $b=17.625(6)$, $c=13.614(3)$ Å. The radical cations align along the c axis at nearly equal spacing forming eclipsed dimers and the dimeric units are stacked with a staggered mode. The electronic spectra of the radical cation and the dimer have been measured in solution and the assignment has been presented with an aid of the MO calculation by Pariser-Parr-Pople method. A charge transfer (CT) band observed in the dimer has been correlated with the charge resonance of unpaired electron between the HOMOs of the radical cations. Polarized reflection spectra of single crystal have been measured with three different crystal planes and the assignment of both the CT and molecular type bands have been confirmed with polarization measurement. The energy and the intensity of the CT band indicate that the unpaired electron is localized on each radical, but the CT configuration is involved significantly. The crystal is an insulator as is expected from the electronic structure; the large U, which is evidenced by the energy of the CT band, and the staggered packing hinders electronic conduction. It implies that a monovalent radical salt is difficult to be metallic unless a mixed valence state is involved.

Tetrathiafulvalene (TTF) and its family are good electron donors[1] which form donor-acceptor complex[2,3] and mixed valence salts as well as monovalence salts depending on the oxidation conditions. The oxidation is carried out either by the chemical method with suitable oxidants[4] or electron acceptor, or by electrochemical method.[5,6] A structural characteristic of organic metal is that the crystal has segregated columns of mixed valence donor or/acceptor stacks.[7] Torrance[8] discussed the relation between the redox-potentials of the donor and acceptor and the degree of charge transfer. The examination of the crystal structures and properties of ion-radical salts and charge transfer compounds is of theoretical and experimental importance to develop new organic metal.

The title compound is a 1 : 1 salt of cation radical of 5,5′-dimethyl-2,2′-bi-1,3-benzodithiol-2-ylidene, which is a dimethyl derivative of dibenzotetrathiafulvalene (DBTTF) and is abbreviated as DMDBTTF in the present paper. Hünig *et al.*[9] reported the oxidation potentials and the electronic spectra of TTF, DBTTF, DMDBTTF, and their cation radicals. The oxidation potential of DMDBTTF is slightly lower than that of DBTTF and the comparison of the structures of these complexes will be interesting. Both DMDBTTF–TCNQ[10] and DBTTF–TCNQ are insulators with alternating donor acceptor stacking.[11–13] DBTTF–$TCNQCl_2$ shows high electrical conductivity because it crystallizes in the segregated stacks of the donor and acceptor.[14,15] DBTTF–DDQ also shows high electrical conductivity and is considered as a mixed valence crystal with a segregated stack of acceptor.[16] DBTTF–$(BF_4)_{0.8}$ has been reported to be a mixed valence and conducting material,[17] but its crystal structure has not been reported yet.

In this paper we report the preparation, the crystal structure and the electronic spectra of DMDBTTF·BF_4 (1 : 1) crystal. We also discuss the electronic structure of the radical monomer and dimer as well as the crystal. The crystal structure found is an unique dimeric type and it is an insulator because the dimer is so stable that the delocalization of unpaired electron is limited within the dimer, and the CT state has fairly large energy characterized by U.

Preparation

DMDBTTF was prepared by the following reaction route using commercial GR. grade toluene-3,4-dithiol.

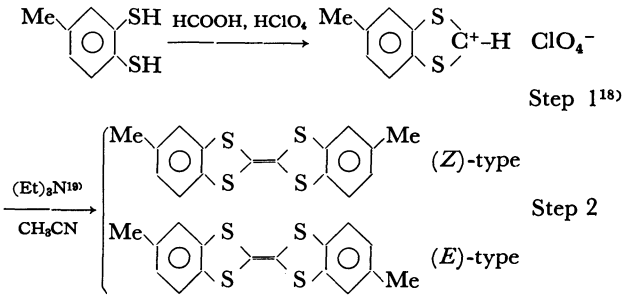

5-Methyl-1,3-benzodithiol-2-ylium perchlorate (4.2 g) obtained in Step 1 was dissolved in 180 ml of acetonitrile. Stirring the solution at 0 °C, acetonitrile solution of triethylamine (2.8 g/10 ml) was added dropwise. Yellow precipitate of DMDBTTF formed immediately. The stirring was continued for 15 min after the addition was completed. The precipitate was collected, washed with acetonitrile and dried. The yields of Steps 1 and 2 were 82 and 93% respectively. The product was purified by column chromatography and recrystallized with benzene and acetonitrile. As shown in above scheme two isomers, (*Z*) and (*E*), are considered for 5,5′-dimethyl-2,2′-bi-1,3-benzodithiol-2-ylidene. But it is not certain whether our product consists of only one isomer or a mixture of isomers.[10]

The electrocrystallization was carried out in the H shaped glass tube with Pt wire electrodes (same results were obtained with Ni electrodes) using dry CH_2Cl_2 solution of DMDBTTF and $(n\text{-Bu})_4N\cdot BF_4$ in inert atmosphere. The yellow color of

†† Permanent address: Institüt für Anorganische Chemie, Universität Heidelberg, West Germany. JSPS post-doctoral fellow 1981—1982 at Nagoya University.

neutral DMDBTTF changed to dark green by electrolysis. Within a few days dark violet prisms covered the (+) electrode, and these crystals were used for X-ray and spectral investigations.

Structural Determination

The crystal shape is shown in Fig. 1. The reflection color of the crystal is dark violet on the (010), silvery purple on the (110) and (1$\bar{1}$0), and brilliant pink on the (001) plane. The Weissenberg photographs showed the space group either Ibam or Iba2 from systematic absences. The reflection data for X-ray structural determination were collected with a Rigaku four-circle diffractometer AFC-5 using graphite-monochromatized Cu $K\alpha$ radiation. Intensities of 1617 reflections were measured up to $\theta=63°$ with the crystal of the size $0.2\times0.08\times0.08$ mm^3. The intensity statistics indicated the structure to be centrosymmetric, therefore the space group was determined as Ibam. The lattice parameters determined using 13 selected reflections are given in Table 1. The structure was solved by Patterson function method. The refinement of the structure was performed by the block-diagonal least-squares method with 1058 independent reflections of $|F_o|\geqq3\sigma$ with anisotropic thermal parameters. The final R index converged to 0.082.** The atomic parameters are shown in Table 2,

TABLE 1. CRYSTAL DATA OF DMDBTTF·BF_4

$C_{16}H_{12}S_4BF_4$	F.W.=419.33
Orthorhombic	Space group: Ibam
$a=14.637(3)$Å, $b=17.625(6)$Å, $c=13.614(3)$ Å	
$V=3512.1$ Å^3	
$D_m=1.584$ Mg m^{-3}, $D_c=1.586$ Mg m^{-3} ($Z=8$)	
μ(Cu $K\alpha$)=51.2 cm^{-1}	

TABLE 2. FRACTIONAL COORDINATES AND THEIR STANDARD DEVIATIONS[a)]

	x	y	z	B_{eq}/Å^2 [b)]
S(1)	0.0603(1)	0.1125(1)	0.1240(2)	3.8
S(3)	0.1404(1)	−0.0393(1)	0.1215(1)	3.8
C(2)	0.0414(4)	0.0157(4)	0.1234(5)	3.5
C(3a)	0.2158(4)	0.0347(4)	0.1272(5)	3.5
C(4)	0.3127(6)	0.0266(5)	0.1311(6)	5.4
C(5)	0.3667(6)	0.0903(5)	0.1365(7)	5.4
C(6)	0.3264(5)	0.1634(5)	0.1394(6)	4.8
C(7)	0.2367(6)	0.1735(5)	0.1365(6)	5.2
C(7a)	0.1778(5)	0.1063(4)	0.1296(5)	3.8
C(m)	0.3916(8)	0.2356(7)	0.1459(10)	9.7
B	0.1240(10)	0.3388(10)	0.0	5.4
F(1)	0.0980(6)	0.2672(4)	0.0	8.2
F(2)	0.0694(6)	0.3948(5)	0.0	10.9
F(3)	0.1933(6)	0.3477(4)	0.0640(9)	15.9

a) The estimated standard deviations are given in parentheses and refer to the last decimal position of respective values. b) $B_{eq}=8\pi^2(U_1^2U_2^2U_3^2)^{1/3}$, where U_i is the root-mean-square deviation in the ith principal axis of the thermal ellipsoid.

** The anisotropic thermal factors and the complete F_o-F_c data are deposited as Document No. 8311 at the Office of the Editor of Bull. Chem. Soc. Jpn.

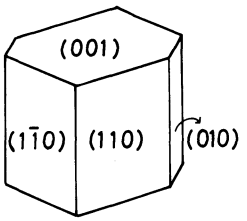

Fig. 1. Crystal shape.

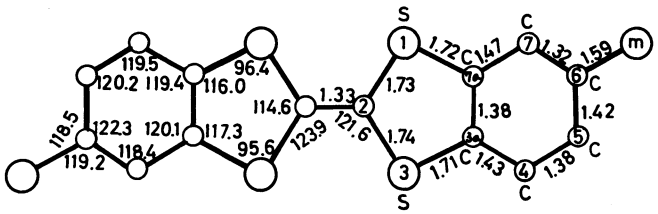

Fig. 2. Bond length (Å) and angles (°) of DMDBTTF$^+$.

and the molecular structure is illustrated in Fig. 2.

The DMDBTTF radical cation is approximately planar, but it is slightly bent towards both ends. The crystallographic two-fold axis coincides with the two-fold axis of the molecule. The least-squares plane for the half of the molecule, the 1,3-benzodithiole ring, is represented as $-0.0348x-0.0371y+0.9987z=1.6100$ (x, y, and z are coordinates in Å referred to the a, b, and c crystal axses, respectively). The deviation of the atoms from the plane is less than 0.04 Å. The dihedral angle between this and the other corresponding plane is 5.8°. The boron atom and two of the four fluorine atoms, F(1) and F(2), of the tetrafluoroborate ion are on the mirror plane and the remaining two fluorine atoms, F(3), are above and below the plane keeping the mirror symmetry. Three residual peaks, which could not be explained by hydrogen atoms, were found in the difference Fourier map. Two of them were around the anion site indicating disordered arrangement of anions. The other one was found in the region to which the methyl group attached to C(5) could be assigned. This suggests the stack includes some molecules whose methyl groups occupy the site on C(5) instead of C(6). However the distance between the methyl group on C(5) and the fluorine atom, F(2), is considerably shorter than normal contact. This may be related to the unusually short bond length of B–F(2), 1.27 Å, and the large anisotropy of thermal ellipsoid of boron atom. Hence, it is considered that the disordered arrangement of the anion is closely connected with that of the cation radical.

The projection of the cations onto three different planes are illustrated in Figs. 3, 4, and 5. Two adjacent cations form an eclipsed dimer whose interplanar spacing at the central bond region is 3.36 Å. The S···S contacts in the dimer are 3.31 and 3.37 Å. These values are comparable with the values found in the eclipsed dimer in TTF·I_3[20] and other integral oxidation state salts.[21,22] The dimers align along the c axis in a staggered mode.

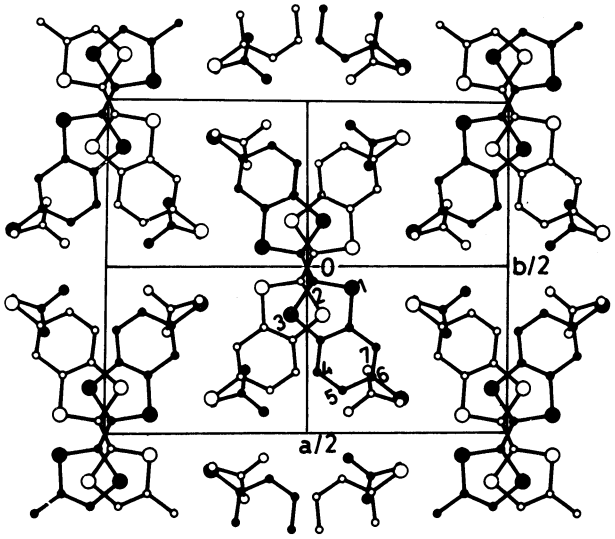

Fig. 3. Projection of the structure onto the (001) plane. The molecules shown with black circles locate above and below the mirror plane at $z=0$. The molecules shown with white circles locate above and below the mirror plane at $z=1/2$. Boron atoms are on the mirror planes.

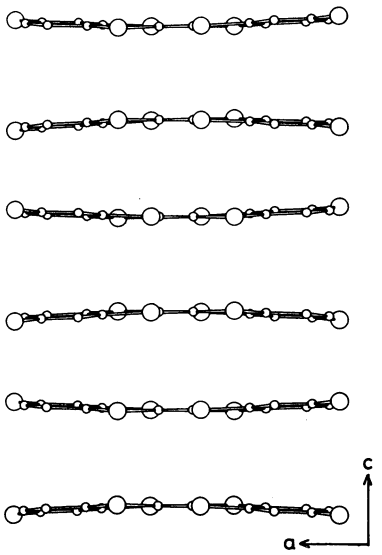

Fig. 4. Projection of the structure onto the (010) plane.

The interplanar spacing between the centers of molecules in the staggered overlapping is 3.45 Å which is almost equal to the interplanar spacing in the dimer. Such a pattern of cation stacking is rather unique as a monocation salt. The structural characteristic will be reflected on the optical and other electronic properties of the crystal.

Electrical Conductivity

The powder conductivity of the crystal is measured with a compressed pellet (diameter=5 mm) under the pressure of 20 kg/cm² at room temperature. The conductivity was $\sigma=5\times10^{-8}\ \Omega^{-1}\ cm^{-1}$. It indicates that the crystal is an insulator. This is reasonable since the crystal is not a mixed valence having an odd electron

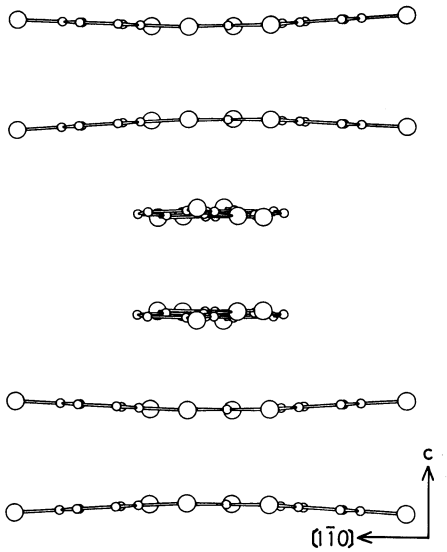

Fig. 5. Projection of the structure onto the (110) plane.

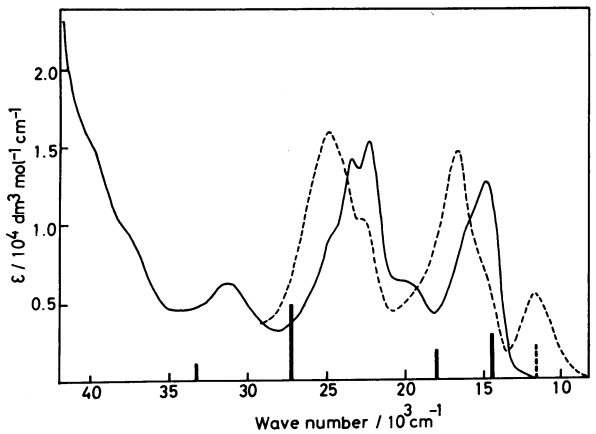

Fig. 6. Absorption spectra of $DMDTTF^+$ in solution (——, 0.26×10^{-5} mol dm^{-3} in CH_2Cl_2 at room temp; ------, 0.67×10^{-3} mol dm^{-3} in CH_3CN at *ca.* −40 °C) and calculated values (——, L1, M1, L2, and M2 for the monomer, from right to left; ------, CT for the dimer).

on each site as is shown by structural analysis and stoichiometry. The electrostatic repulsive energy is big enough to prevent electrons moving freely in the crystal. This point will be discussed below from optical evidence and its theoretical analysis.

Electronic Spectra of the Cation Radical in Solution

Electronic absorption spectra of the cation radical salt in monomeric and dimeric states measured in dichloromethane and in acetonitrile solutions, respectively, are shown in Fig. 6. As reported by Hünig *et al.*,[9] the neutral molecule has only a weak absorption band in the region below 25000 cm^{-1}, therefore the strong bands observed at 14600 and 22000—24000 cm^{-1} region are attributed to the radical monomer. The monomer has no absorption band in the region between 5000—11000 cm^{-1}. The electronic spectra of the dimer

was already reported by Hünig *et al.*,[9] and we confirmed their result more clearly by measuring the spectra at lower temperature as is shown in Fig. 6. In the dimeric state, the CT band between the radicals is observed at 11600 cm^{-1}. The bands at 14600 and 22000—24000 cm^{-1} in the monomeric state are shifted by 2000—2600 cm^{-1} to higher energy upon dimerization. Similar spectral change was reported in TTF^+ dimer.[23]

Calculation of the Excited States of the Monomer

In order to give an assignment of radical monomer spectra, Pariser-Parr-Pople type calculation for the open shell system was performed. The computer program developed in our laboratory based on the scheme of Lowitz[24] was used for the calculation. The value of the valence state orbital energies and the one-center Coulomb integrals used in our calculation were as follows; $U_{cc}=-11.22$ eV, $(CC|CC)=10.60$ eV, $U_{ss}=-9.16$ eV, $(SS|SS)=10.01$ eV. The values for U_{cc} and $(CC|CC)$ are the standard values. The value of $(SS|SS)$ has been evaluated from the data of Hinze and Jaffe[25] by the use of Pariser-Parr approximation. The value of U_{ss} was selected in order that the result of the calculation might be in reasonable agreement with the observed data. The core resonance integral β was calculated by the use of Wolfsberg and Helmholz formula,[26] where the proportional constant was set as $K=0.39$. All calculations were carried out using the single exponent Slater AO. The results of the calculation on energies, intensities and polarizations are shown in Table 3 and illustrated in Fig. 6. The bands at 14600 and 22000—24000 cm^{-1} are found to be polarized in the direction of the molecular long axis (L1 and L2), while the 19500 and 31500 cm^{-1} bands are polarized in the direction of the molecular short axis (M1 and M2). The agreement of the calculated and observed values was satisfactory particularly on sequence of transition energies and intensities, and on polarizations. The polarization characteristics were all confirmed by the polarized spectral measurement of the single crystal as is discussed below.

Table 3. Electronic excited states of radical cation

	Monomer spectra in solution		Open sheell P-P-P caluculation		
State	Energy/10^3 cm^{-1}	f	Energy/10^3 cm^{-1}	Pol.	f
L1	14.6	0.19	14.5	L	0.28
	16.0				
M1	19.5	0.05	17.9	M	0.18
L2	22.1	0.22	27.3	L	0.52
	23.4				
	24.8				
M2	31.1	0.13	33.3	M	0.11
	Dimer spectra in solution		Calculated excited states of dimer		
CT	11.6	0.12	11.6	N	0.17
L1	16.6	0.40	16.7	L	0.38
M1	19.6	0.09			
L2	25.0	0.68	24.2	L	0.44

Theoretical Treatment of the Dimer Spectra

Before going to the discussion of the crystalline spectra, we will consider the electronic structure of the dimer, since molecules are paired tightly in the crystal forming the eclipsed dimer. The molecular overlap integral between the molecules in the eclipsed pair is 0.0260, while that between the molecules in the staggered pair is 0.0015, therefore the molecular interaction is much larger in the eclipsed pair than in the staggered pair. Under this condition the crystalline electronic states can be described as an assembly of the eclipsed dimer.

The electronic structure of the cation radical dimer can be described by Hubbard Hamiltonian as was shown in our earlier paper on TCNQ complexes.[7] The electronic states are factored into a symmetric and an antisymmetric states under the inversion symmetry of the dimer. Matrix elements of the secular equations are given as follows.

$$\begin{vmatrix} 0 & 2t_{mm} & 0 \\ & U & \sqrt{2}\,t_{mm-1} \\ & & \Delta-\delta \end{vmatrix} \begin{matrix} \text{G} \\ \text{CT}^{(+)} \\ \text{LE}^{(+)} \end{matrix} \qquad \begin{vmatrix} U & \sqrt{2}\,(t_{mm-1}+2\text{D}) \\ & \Delta+\delta \end{vmatrix} \begin{matrix} \text{CT}^{(-)} \\ \text{LE}^{(-)} \end{matrix}$$

Symmetric state Antisymmetric state

The dipole transition from the G to the $CT^{(-)}$ and $LE^{(-)}$ states are allowed by the selection rule. The diagonal energy of the CT state is given as $U=\eta(U^{pp}_{mm}-U^{pq}_{mm})$, where U^{pp}_{mm} is the Coulomb repulsion energy between two electrons on the (mth) MO (HOMO) of the same molecule (p), and U^{pq}_{mm} is the one between two electrons on the HOMOs of the adjacent molecule (p and q). The numerical values of U^{pp}_{mm} and U^{pq}_{mm} were calculated as 4.12 and 2.44 eV respectively, by the use of Nishimoto-Mataga potential. The difference between these two terms was 1.68 eV. Δ is the energy of the LE state in the monomer (1.81 eV for the L1 state and 2.74 eV for the L2 state). η is the screening constant due to the electronic polarization. t_{mm} in the off-diagonal matrix element is a transfer integral, the numerical value of which is estimated by the relation $t_{mm}=-kS_{mm}$ where S_{mm} is the overlap integral between the HOMOs m, and k is an empirical parameter. t_{mm-1} and D (the dipole interaction energy between the $CT^{(-)}$ and $LE^{(-)}$ states) can be ignored because the symmetries of the states are different and the transition moments are orthogonal to each other. The diagonal energy for the $LE^{(-)}$ states, Δ, are lifted by the amount δ, the exiton type dipole-dipole interaction, which was not explicitly described in the earlier paper.[7] The numerical value of δ was evaluated as 0.07 eV, by a dipole calculation based on a weak coupling model scaled by the transition density method[27] for the L1 and the L2 bands. When the set of parameters $\eta=0.74$ and $k=10.0$ eV were chosen to estimate U and t, the calculated transition energies from the G state to the $CT^{(-)}$, $L1^{(-)}$, and $L2^{(-)}$ states are in good agreement

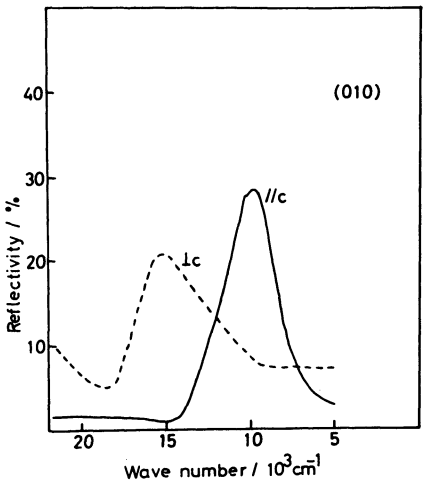

Fig. 7a. Polarized reflection spectra on the (010) plane.

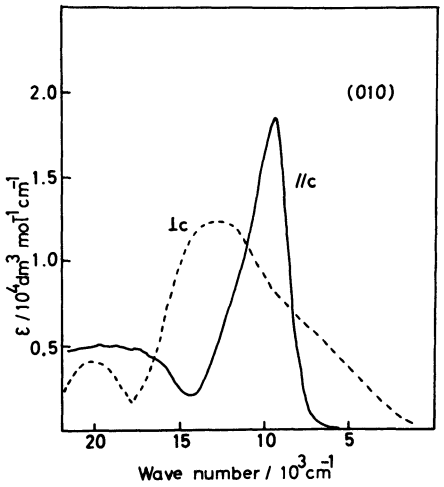

Fig. 7b. Polarized absorption spectra (K-K transformed) on the (010) plane.

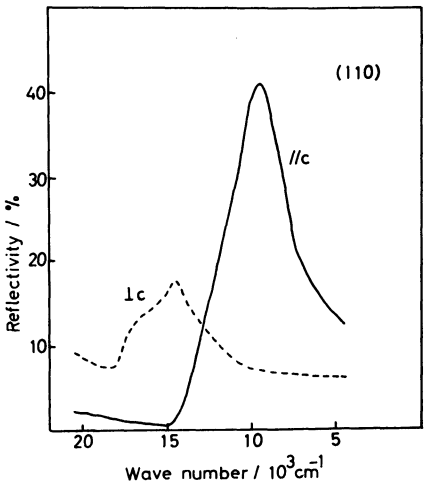

Fig. 8a. Polarized reflection spectra on the (110) plane.

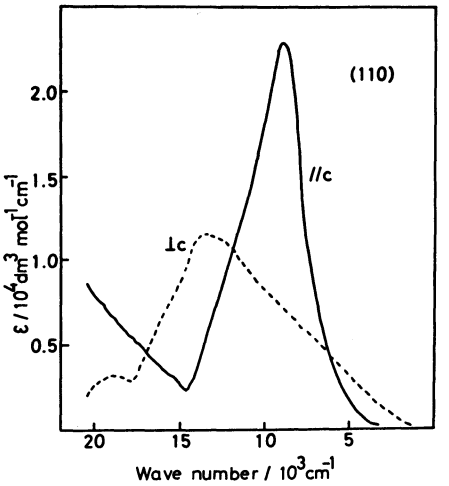

Fig. 8b. Polarized absorption spectra (K-K transformed) on the (110) plane.

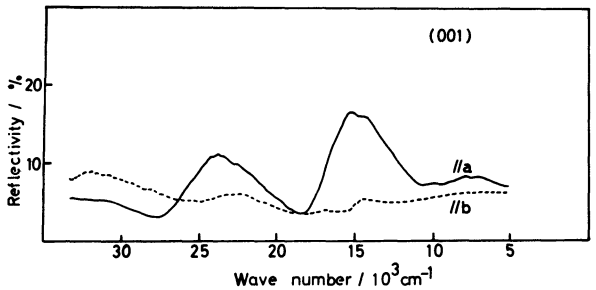

Fig. 9a. Polarized reflection spectra on the (001) plane.

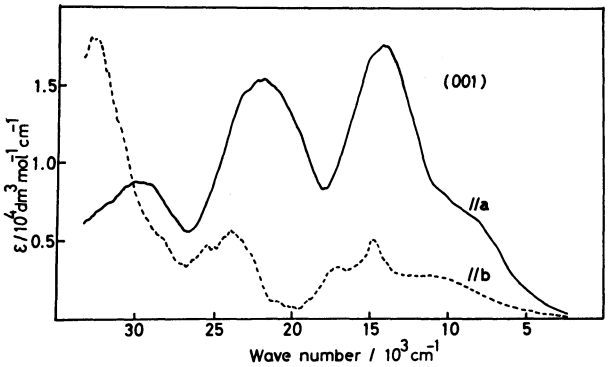

Fig. 9b. Polarized absorption spectra (K-K transformed) on the (001) plane.

with the observed energies of the dimer in solution (Table 3). The assignment of the dimer spectra is confirmed by this calculation.

Electronic Spectra of Crystals

The crystalline reflection spectra were measured with the crystals of the size about $0.3\times0.3\times0.6$ mm^3 for the (010) and (110) faces and $0.5\times0.3\times0.2$ mm^3 for the (001) face by the use of a polarized microspectrophotometer. The results are shown in Figs. 7—9. The calculation of the excited states were carried out for these planes by summing up the dipole-dipole interaction over molecules within 200 Å radius and 30 Å depth in order to consider the directional dispersion of the exciton states.[28,29] The transition energies of the dimer

in solution were used for the diagonal energies of the CT, L1, M1, and L2 bands. However, we made the correction for the standard of the state energies by $-1000\ cm^{-1}$ for the CT level and $-2000\ cm^{-1}$ for other levels by taking into account the crystalline polarization effect. For the calculation of the off-diagonal energies of the dipole-dipole interaction, the length of transition moment estimated from the solution spectra of the dimer for each bands were used. All calculations were based on the dimer unit and the transition moments are placed in the center of the dimer. By this procedure the second order mixing and the exaggeration of the band shift were avoided. The results of calculation are tabulated in Table 4 and the calculated transition energies are compared with the observed crystalline spectra in the following.

In Figs. 4 and 5 the projection of molecules onto the (010) and (110) planes are illustrated. On these planes, the CT band is expected along the c axis. In Figs. 7 and 8 the reflectivities, Kramers-Kronig transformed spectra are illustrated. Although the absolute magnitude of reflectance is different between the planes, the CT band is found with a great intensity only along the c axis. The intensity is enhanced in the crystal by a factor of 2—4 as compared with that of the dimer in solution. This gives an evidence of an increase of the intermolecular CT interaction in the crystal. The observed CT energies were at 9000—9400 cm^{-1}, while the calculated values were 9000—9100 cm^{-1}, hence the agreement between the calculated and observed values was quite satisfactory. The result shows that the electron electron repulsion U is predominant in determining the energy level of the CT band in the monovalence radical salt. A similar spectral characteristic was reported by Kuroda *et al.*[30] and by Torrance *et al.*[23] on several TTF salts.

For the (001) plane the projection of molecules is shown in Fig. 3 and the reflection spectra and Kramers-Kronig transformation to molar absorption coefficent are shown in Fig. 9. The long-axis of the molecule is at the angle of 24.5° with the a axis, therefore the L type bands should be stronger along the a axis than the b axis, while that of the M type bands are stronger along the b axis. The Kramers-Kronig transformed spectra are in perfect agreement with this expectation that the L1 band appearing at 15000 cm^{-1} region and the L2 band at 22000 cm^{-1} range are stronger along the a axis than the b axis, while the M1 and M2 bands found at 17000 and 31000 cm^{-1}, which are correlated with the solution bands at 19500 cm^{-1} and 31500 cm^{-1}, are stronger along the b axis than along the a axis. The observed band position for the (001) plane are well explained by the calculation of the exciton splitting, however, the Davydov splitting for the L1 band is reversed in order. The calculated intensities shown in Table 4 are larger by a factor of 2, but the order of its size is in agreement with the observed ones. Although the intermolecular CT transition is not expected with the (001) plane since it is polarized along the c axis, but the absorption tail is found around at 10000 cm^{-1} region, and it may be due to the admixture of the c axis transition in this measurement because the incident beam has a glazing angle of 4—11°, hence it may have a slight component along the c axis.

Table 4. Polarized crystalline spectra

Plane	State	Pol. axis	Energy/$10^3\ cm^{-1}$		f	
			Obsd	Calcd	Obsd	Calcd
(001)	L1	a	14.2	14.8	0.50	0.91
		b	14.7	13.3	0.09	0.22
	M1	a		17.4		0.07
		b	17.0	17.6	0.05	0.24
	L2	a	22.5	23.2	0.33	1.81
		b	22.0	22.0	0.17	0.28
	M2	a	31.0		0.14	
		b	29.5		0.48	
	CT	c	—	10.3	—	0.35
(110)	CT	c	9.0	9.0	0.50	0.31
	L1	[1$\bar{1}$0]	13.5	16.2	0.36	0.23
				14.2		0.11
(010)	CT	c	9.4	9.1	0.23	0.32
	L1	a	13.0	14.8	0.43	0.91

Thus the assignment of electronic transitions is confirmed by the polarized spectral measurement and the calculation of exciton band shift for each planes.

Conclusion

$(DMDBTTF)^+$ radical obtained by electrochemical oxidation of neutral molecule crystallizes with BF_4^- forming a pseudo-one-dimensional crystal with unpaired electrons on each site. The radicals form eclipsed dimers in the crystal, and the dimers are aligned along the crystalline c axis with a staggered mode. This type of molecular packing may be occurred through a steric hindrance of the methyl groups at both ends. In this structure the transfer integral for the eclipsed pair (t_1) is much larger than that of the staggered pair (t_2), therefore the electronic structure of the dimer is conserved in the crystal. Namely the electronic spectra of the crystal is almost same with that of the dimer in solution, except that the molecular bands are red shifted and the CT band is enhanced. It reflects that the molecular character of the dimer is reserved in the crystal in spite of the CT interaction is conceivable between the dimer. It is reasonable since t_2 is negligibly small as compared to t_1.

The energy of the CT band gives an estimate of U for the dimer interaction, where the value of U is the change of repulsive energy of electrons accompanied with the charge transfer. It is significantly large as $U=1.24$ eV ($\simeq 5t_1$). The CT configuration in the ground state is estimated as 12% from the normalized wavefunction. A fairly large oscillator strength of the CT band is accounted for by this contribution. The crystal is an insulator in spite of apparent one-dimensional stacking of radicals, because U is large as usually found in monovalence salts. Moreover, the one-dimensional equality of the electronic structure is not realized since $t_1 \gg t_2$. Anyway the mixed valence state is most important to find organic metal.

All computations were carried out at the Nagoya University Computation Center; NUNICS program was used for crystal structure analysis.

The authors thank to JSPS for the fellowship to K. Dietz.

References

1) F. Wudl, G. M. Smith, and E. J. Hufnagel, *Chem. Commun.*, **1970**, 1453.
2) J. Ferraris, D. O. Cowan, V. Walatka, Jr., and J. H. Perlstein, *J. Am. Chem. Soc.*, **95**, 948 (1973).
3) A. J. Heeger, "Highly Conducting One-Dimensional Solids," ed by J. T. Devreese, R. P. Evrard, and V. E. van Doren, Plenum Press, New York (1979), p. 69.
4) F. Wudl, D. E. Schafer, W. M. Walsh, Jr., L. W. Rupp, F. J. DiSalvo, J. V. Waszczak, M. L. Kaplan, and G. A. Thomas, *J. Chem. Phys.*, **66**, 377 (1977).
5) F. B. Kaufman, E. M. Engler, D. C. Green, and J. Q. Chambers, *J. Am. Chem. Soc.*, **98**, 1596 (1976).
6) K. Bechgaard, C. S. Jacobsen, K. Mortensen, H. J. Pedersen, and N. Thorup, *Solid State Commun.*, **33**, 1119 (1980).
7) J. Tanaka, M. Tanaka, T. Kawai, T. Takabe, and O. Maki, *Bull. Chem. Soc. Jpn.*, **49**, 2358 (1976).
8) J. B. Torrance, *Acc. Chem. Res.*, **12**, 79 (1979).
9) S. Hünig, G. Kiesslich, H. Quast, and D. Scheutzow, *Justus Liebigs Ann. Chem.*, **1973**, 310.
10) G. S. Bajwa, K. D. Berlin, and H. A. Pohl, *J. Org. Chem.*, **41**, 145 (1976).
11) R. P. Shibaeva and O. V. Yarochkina, *Dokl. Akad. Nauk SSSR*, **222**, 91 (1975).
12) H. Kobayashi and J. Nakayama, *Bull. Chem. Soc. Jpn.*, **54**, 2408 (1981).
13) T. J. Kistenmacher, T. J. Emge, F. M. Wiygul, W. A. Bryden, J. S. Chappell, J. P. Stokes, L-Y. Chiang, D. O. Cowan, and A. N. Bloch, *Solid State Commun.*, **39**, 415 (1981).
14) C. S. Jacobsen, H. J. Pedersen, K. Mortensen, and K. Bechgaard, *J. Phys. C*, **13**, 3411 (1980).
15) H. Soling, G. Rindorf, and N. Thorup, *Acta Crystallogr., Sect. B*, **37**, 1716 (1981).
16) J. J. Mayerle and J. B. Torrance, *Bull. Chem. Soc. Jpn.*, **54**, 3170 (1981).
17) I. V. Krivoshei, V. P. Babiyczuk, I. M. Guella, I. F. Golovkina, N. V. Mansia, V. A. Starodub, and S. A. Chueva, *Phys. Status Solidi A*, **50**, K197 (1978).
18) L. Soder and R. Wizinger, *Helv. Chim. Acta*, **42**, 1733 (1959).
19) F. Wudl, M. L. Kaplan, E. J. Hufnagel, and E. W. Southwick, Jr., *J. Org. Chem.*, **39**, 3608 (1974).
20) R. C. Teitelbaum, T. J. Marks, and C. K. Johnson, *J. Am. Chem. Soc.*, **102**, 2986 (1980).
21) B. A. Scott, S. J. La Placa, J. B. Torrance, B. D. Silverman, and B. Welber, *J. Am. Chem. Soc.*, **99**, 6631 (1977).
22) K. Yakushi, S. Nishimura, T. Sugano, H. Kuroda, and I. Ikemoto, *Acta Crystallogr., Sect. B*, **36**, 358 (1980).
23) J. B. Torrance, B. A. Scott, B. Welber, F. B. Kaufman, and P. E. Seiden, *Phys. Rev. B*, **19**, 730 (1979).
24) D. A. Lowitz, *J. Chem. Phys.*, **46**, 4698 (1967).
25) J. Hinze and H. H. Jaffé, *J. Am. Chem. Soc.*, **84**, 540 (1962).
26) M. Wolfsberg and L. Helmholtz, *J. Chem. Phys.*, **20**, 837 (1952).
27) J. N. Murrell and J. Tanaka, *Mol. Phys.*, **7**, 363 (1964).
28) M. R. Philpott, *J. Chem. Phys.*, **58**, 588 (1973).
29) J. Tanaka, M. Tanaka, and M. Hayakawa, *Bull. Chem. Soc. Jpn.*, **53**, 3109 (1980).
30) T. Sugano, K. Yakushi, and H. Kuroda, *Bull. Chem. Soc. Jpn.*, **51**, 1041 (1978).